Application of Semirigid Vibrating Rotor Target Model to the Reaction of $O(^3P) + CH_4 \rightarrow CH_3 + OH$†

Ming-Liang Wang, Yi-Min Li, and John Z. H. Zhang*

Department of Chemistry, New York University, New York, New York 10003

Received: October 13, 2000; In Final Form: November 29, 2000

In this paper, the SVRT (semirigid vibrating rotor target) model has been applied to study the reaction of $O(^3P) + CH_4 \rightarrow CH_3 + OH$ using the time-dependent wave packet (TDWP) method. Employing the basic SVRT model, quantum dynamics calculation for any atom−polyatom reaction involves only four mathematical dimensions (4D). The reaction probability, cross section, and rate constant from the initial ground state are calculated for the title reaction on potential energy surfaces of Corchado et al. (C-T) and Jordon and Gilbert (JG). The calculated reaction probabilities on the C-T surface are significantly smaller than those calculated on the JG surface. The difference in barrier height is insufficient to account for the difference in the magnitude of reaction probabilities on two surfaces. Instead, global contour plots show that the C-T surface appears to have incorrect contour lines near the reaction region which tend to help reflect the wave packet back toward the entrance channel. On the other hand, our calculated rate constants on the JG surface are in good agreement with experimental measurements over a range of temperatures.

I. Introduction

Currently, exact quantum mechanical approaches can be used to study dynamics of chemical reactions involving no more than four atoms.[1−7] For polyatomic reactions beyond tetraatomic systems, however, one has to employ dynamical approximations in order to study their dynamics.[8,9] As examples, some of the approximate dynamical methods have been applied to the benchmark H_2OH reaction and some reasonable results have been obtained from these approximate calculations.[10−13] However, the results of many of these approximate methods are generally mixed and their suitability to treat general polyatomic reactions beyond tetraatomic systems are not yet known.

Recently, the SVRT (semirigid vibrating rotor target) model has been proposed as a general theoretical model for practical dynamics calculation of chemical reactions involving polyatomic molecules.[14] In the SVRT model, the reacting (target) polyatomic molecule is treated as a semirigid vibrating rotor whose spatial motion is accurately treated as a three-dimensional rotor. As a result of accurate treatment of spatial rotation, the SVRT model preserves the correct stereodynamics of the reaction system which plays an important role in polyatomic reactions. Using the SVRT method, excellent reaction probability, cross section, and rate constant have been obtained for the benchmark $H + H_2O$ reaction when compared with the exact quantum results.[15] The SVRT model has also been applied recently to study the dynamics of the six-atom $H + CH_4$ reaction.[16] On the basis of its attractive features and numerical test results, we believe that the SVRT model provides a general and practical approach for computational study of reaction dynamics involving polyatomic molecules.

In this paper, we use the SVRT model to study another six-atom reaction, $O(^3P) + CH_4 \rightarrow OH + CH_3$. The reaction $O(^3P) + CH_4 \rightarrow OH + CH_3$ is a prototype hydrogen abstraction reaction. It is a primary step in methane combustion. The kinetics of the reaction has been extensively studied both experimentally and theoretically.[17−25] Theoretical dynamics studies have also been reported for this reaction.[23,26−28] We note in particular the reduced dimensionality quantum scattering calculations by Clary[26,27] and Yu and Nyman.[28] Clary employed a 3D rotating bond approximation (RBA) to carry out the dynamics calculation using the potential surface of ref 21 (C-T surface). Yu and Nyman used a 4D RBU (rotating bond umbrella) model and employed a newer potential surface by Espinosa-Garci.[22] The RBU model is an extension of the RBA model by including an extra umbrella vibrational mode of CH_4.[28] Both studies use time-independent hyperspherical coordinate approach, and the rate constant obtained by Yu and Nyman agrees better with experimental measurement. Because of the nature of both models, neither calculation seems capable of giving correct initial state-selected reaction probabilities. In the following, we employ the SVRT model to carry out time-dependent quantum dynamics calculation for the title reaction. Since the SVRT model treats molecular rotations correctly, it gives correct stereodynamics information for polyatomic reactions and individual reaction probabilities. Our dynamics calculations are performed on two potential energy surfaces (PES): that of ref 22 (C-T) and the PES for $H + CH_4$ of ref 29 (JG). It is noted that both $O(^3P) + CH_4$ and $H + CH_4$ reactions have similar reaction barriers, in both location and height of the barrier. Therefore, it is natural to use the PES of $H + CH_4$ to study the $O(^3P) + CH_4$ reaction. Since no product state distribution is obtained in our calculation, incorrect asymptotic behavior of the JG PES in the product channel for the title reaction is immaterial in the present study.

This paper is organized as follows. Section II provides brief theoretical treatment of the SVRT model for application to the $O + CH_4$ reaction as well as time-dependent formalism for wave packet propagation. Numerical results including reaction probability, cross section, and rate constant obtained from both potential energy surfaces and their discussions are given in section III. Comparison with other theoretical calculations and

† Part of the special issue "William H. Miller Festschrift".

10.1021/jp003768e CCC: $20.00
Published on Web 02/01/2001

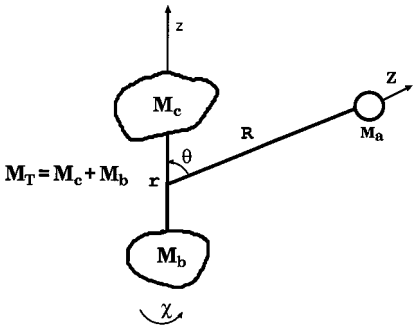

Figure 1. SVRT model for atom−polyatom reaction. The coordinate r is the distance between the center-of-mass of fragment B and C, R the radial distance between atom A and the center-of-mass of T, and θ the polar angle. The angle χ is the rotational angle of the target molecule T about its molecular z-axis.

with experimental measurement, whenever possible, are also given in this section. Section IV concludes.

II. Basic SVRT Model for Atom−Polyatom Reaction

A. Hamiltonian. The SVRT model has recently been applied to H + H_2O[15] and H + CH_4[16] reactions. In the SVRT model for the atom−polyatom reaction, the Hamiltonian for reactive collision between an atomic projectile A and the SVRT molecule T can be expressed as[14]

$$\hat{H}_{ap} = -\frac{\hbar^2}{2\mu}\frac{\partial^2}{\partial R^2} + \frac{\hat{\mathbf{L}}^2}{2\mu R^2} + \hat{H}_T + V \tag{1}$$

where μ is the reduced translational mass,

$$\mu = \frac{M_A M_T}{M_A + M_T} \tag{2}$$

R the relative radial distance between the CMS (center-of-mass) of A and T, and $\hat{\mathbf{L}}$ the orbital angular momentum operator.

The internal Hamiltonian $\hat{H}_T$ describing the SVRT molecule T is given by[14]

$$\hat{H}_T = \frac{1}{2}\sum_{ij}\hat{\Pi}_i G_{ij}\hat{\Pi}_j - \frac{\hbar^2}{2\mu_T}\frac{\partial^2}{\partial r^2} + V_T(r) \tag{3}$$

where r is the radial distance, $V_T(r)$ is the interaction potential, and μ_T is the reduced mass between B and C fragments of molecule T

$$\mu_T = \frac{M_B M_C}{M_B + M_C} \tag{4}$$

with $M_T = M_B + M_C$. The first term in eq 3 indicates the rotational energy of the semirigid rotor in which $\hat{\Pi}_i$ is the projection of the angular momentum operator of molecule T along the body-fixed (BF) axis i ($i = x, y, z$). Here the z axis is chosen to point along the intermolecular distance between fragments B and C of the target. On the other hand, the x or y axis can be chosen arbitrarily. For convenience, one could choose the x, y axes such that the momentum of inertia I_{ij} ($i, j = x, y, z$) is diagonal. One notes that the rotation constant tensor G_{ij} in eq 3 depends on coordinate r. The SVRT Jacobi coordinates for the atom−polyatom model are illustrated in Figure 1 with specification for O + CH_4 reaction in Figure 2.

B. TD Wave Packet Approach. The numerical calculation for atom−polyatom reactive collision using the SVRT Hamiltonian of eq 1 is carried out using the time-dependent (TD) wave packet approach for the reaction.[30] In the TD approach, one solves the TD Schrödinger equation

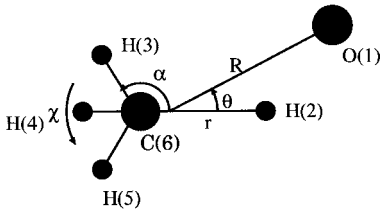

Figure 2. Specification of the SVRT model for O(^{3}P) + CH_4 reaction. The CH_3 is fixed at the transition state geometry with C−H bond fixed at 1.094 Å and $\alpha = 107.45°$.

$$i\hbar\frac{\partial}{\partial t}\Psi(t) = H\Psi(t) \tag{5}$$

with the Hamiltonian defined in eq 1. With an appropriate choice of basis set, the expansion of $\Psi(t)$ can take the form[14,15]

$$\Psi(t) = \sum_{pvjKn} u_p^v(R)\, Z_{jK(n)}^{JM}(\Omega,\theta,\chi)\, \phi_v(r) C_{pvjKn}(t) \tag{6}$$

where $u_p^v(R)$ is the translational basis function whose definition is given in ref 4, $\phi_v(r)$ is the vibrational basis function given by the solution of the one-dimensional eigen equation

$$\left[-\frac{\hbar^2}{2\mu_T}\frac{\partial^2}{\partial r^2} + V_T(r)\right]\phi_v(r) = \epsilon_v\phi_v(r) \tag{7}$$

and $Z_{jK(n)}^{JM}(\Omega,\theta,\chi)$ is the body-fixed (BF) total angular momentum eigenfunction. For the atom−polyatom system, the angular momentum eigenfunction is given by[14,15]

$$Z_{jK(n)}^{JM}(\Omega,\theta,\chi) = \bar{D}_{MK}^{J}{}^*(\Omega)\bar{d}_{Kn}^{j}(\theta)\frac{1}{\sqrt{2\pi}}e^{in\chi} \tag{8}$$

The TD wave function is propagated by employing the split-operator method[31]

$$\Psi(t+\Delta) = e^{-i\hat{H}_0\Delta/2}e^{-i\hat{U}\Delta}e^{-i\hat{H}_0\Delta/2}\Psi(t) \tag{9}$$

where the operator $\hat{H}_0$ can be defined as

$$\hat{H}_0 = -\frac{\hbar^2}{2\mu}\frac{\partial^2}{\partial R^2} - \frac{\hbar^2}{2\mu_T}\frac{\partial^2}{\partial R^2} + V_T(r) \tag{10}$$

The generalized potential operator U is defined as

$$\hat{U} = \hat{H}_{rot} + \hat{V} \tag{11}$$

where $\hat{H}_{rot}$ is the rotation Hamiltonian

$$\hat{H}_{rot} = \frac{\hat{\mathbf{L}}^2}{2\mu R^2} + \frac{1}{2}\sum_{ij}\hat{\Pi}_i G_{ij}\hat{\Pi}_j \tag{12}$$

C. Rovibrational Eigenfunction. The initial rovibrational eigenfunction of the reagent CH_4 in the SVRT model, denoted by $\psi_{vn}^{jm}(\Omega_T, r)$ with three Euler angles Ω_T and vibrational coordinate r, is obtained by solving the Schrödinger equation

$$\left[\frac{1}{2}\sum_{ij}\hat{\Pi}_i G_{ij}\hat{\Pi}_j - \frac{\hbar^2}{2\mu_T}\frac{\partial^2}{\partial r^2} + V_T(r)\right]\psi_{vk}^{jm} = E_{vjk}\psi_{vk}^{jm} \tag{13}$$

Here j and m are, respectively, quantum numbers of the angular

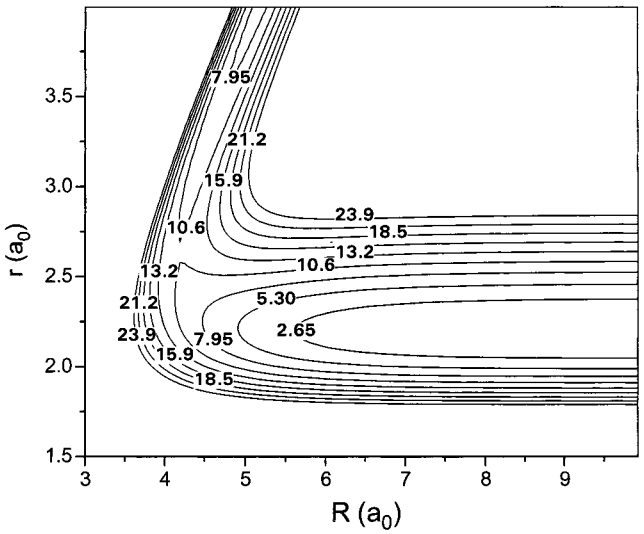

Figure 3. Contour plot of C-T PES of ref 29 where the angle θ is set to zero (collinear approach).

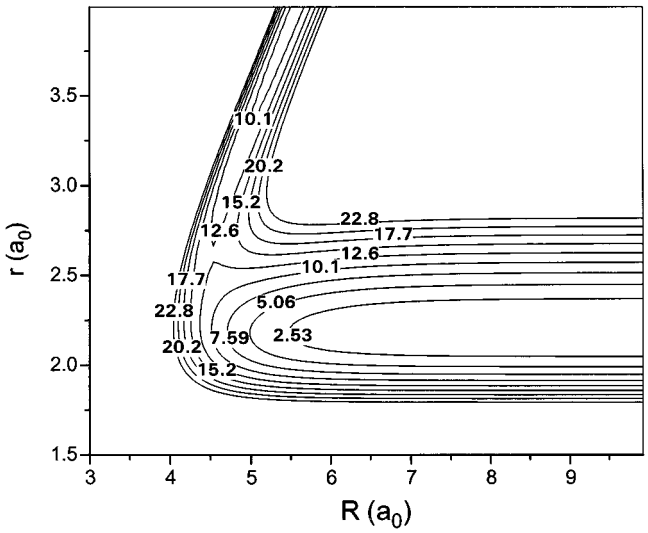

Figure 4. Same as Figure 3 but for JG PES of ref 21.

momentum and its projection on the space-fixed (SF) Z axis, k is an additional angular momentum label and v is the label for vibrational state.

III. Numerical Application to the $O(^3P) + CH_4$ Reaction

In the treatment of the basic SVRT model,[14] only four of the 12 internal coordinates for the $O(^3P) + CH_4$ system are treated explicitly in the dynamics calculation. The polyatomic molecule $H-CH_3$ is treated as a semirigid vibrating rotor that consists of one fragment of H atom and another of CH_3, as shown in Figure 2. Using the basic SVRT model, the internal coordinates are fixed for the CH_3 fragment. Also by preserving the C_{3v} symmetry of $H\cdots CH_3$, only two parameters are left to be determined; the spectator CH bond length in the CH_3 group and bond angle α between the reactive CH bond and spectator CH bond, as shown in Figure 2. The above two parameters change slightly from reactant to transition state, it is reasonable to choose their values corresponding to that at the transition state.

In the current SVRT study, we employ two potential energy surfaces (PES) to perform dynamics calculations. The potential energy surface of ref 21 (C-T PES) has a reaction barrier of about 12.6 kcal/mol as shown in Figure 3. In comparison, the barrier height on the PES of ref 29 (JG PES) is about 10.7 kcal/mol, as shown in Figure 4. Those values are more or less within the estimated experimental activation energy (including zero point energy) of 8.7−11.7 kcal/mol.[32] Although both surfaces are similar in many respects, some differences can be observed in contour plots in Figures 3 and 4. In Figure 4, the energy of the JG surface rises slowly as the system moves from the entrance toward reaction barrier. In Figure 3, however, the energy rise of the C-T PES is quite steep and the contour lines do not "bend" toward the saddle point. This makes the reaction more difficult on the C-T PES surface than on the JG PES surface. On the basis of our experience, we tend to favor the JG PES whose contour lines appear to be more realistic. As will be shown later, the different topologies of the two surfaces are responsible for giving vastly different reactivities on two surfaces.

After the 4D PES is determined by fixing the geometry of CH_3 described above, the 4D TD dynamics calculation is carried out. A total of 30 vibrational basis functions are used in the expansion for the r dependence of the wave function. The maximum rotational quantum number of the CH_4 molecule included in the basis expansion is $j = 35$, which is sufficient to give converged result. Moreover, a total of 120 sine basis functions spanning R from 3.0 to 10.5 Bohr are used in the wave function expansion.

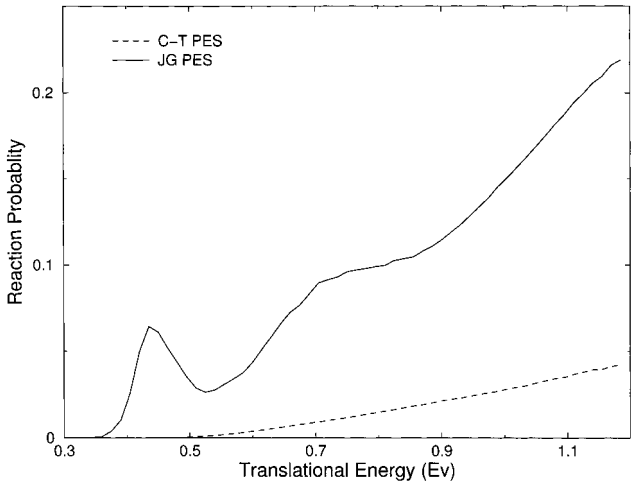

Figure 5. Energy dependence of reaction probability from initial ground state for total angular momentum $J = 0$. The solid line is the result on JG PES and the dashed line the result on C-T PES.

Figure 5 shows the calculated total reaction probability from the initial ground state of CH_4 as a function of collision energy for total angular momentum $J = 0$ on both C-T and JG PES. One should note that since the hydrogen atom in the reagent CH_4 is treated as distinguishable, the reaction probability from the dynamics calculation is multiplied by a factor of 4 to account for equal and independent contribution to reaction probability from all the hydrogen atoms in CH_4. Thus, the results in Figure 5 already include a factor of 4. As shown in Figure 5, the reaction probabilities calculated on the C-T PES are significantly smaller than those on the JG PES. In particular, the difference in the energy dependence of reaction probabilities in Figure 5 on two surfaces could not be simply explained by the 2 kcal/mol difference in barrier height. Our wave packet calculation shows clearly that the wave packet on the C-T PES reflects back quickly from the region of potential barrier, much more than on the JG PES. This can be explained by the contour plot of the C-T PES in Figure 3 in which contour lines "bend" downward away from the saddle point instead of "bending"

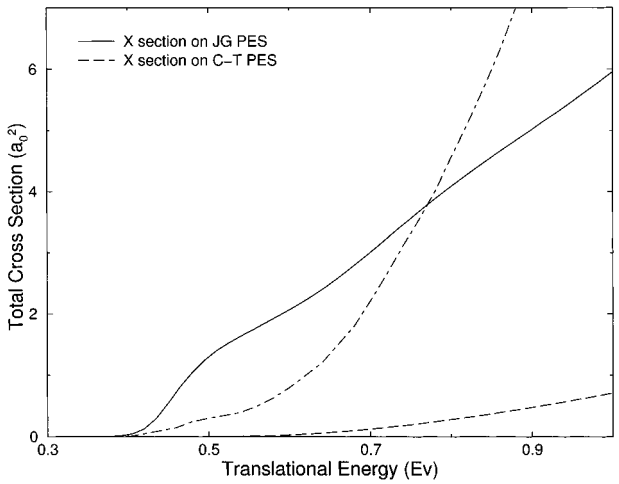

Figure 6. Similar to Figure 5 but for the energy dependence of reaction cross section. Here the theoretical RBA result of ref 26 is given as dot−dashed line.

upward toward the saddle point. This is an indication that the C-T PES is problematic for dynamics calculation.

For calculation result on the JG PES, we note that the quantum tunneling effect is quite pronounced, as shown by the solid line in Figure 5. There is already measurable reaction probability at energies below the barrier. This is expected since this is a typical heavy−light−heavy reaction in which the light hydrogen atom hops between two heavy masses. In addition, the reaction probability shows a peak near the collision energy of 0.43 eV, which is very close to the reaction barrier on the JG PES. Although we are quite sure that tunneling must be involved here, we do not know the exact cause of this peak. Whether it corresponds to any physical resonance state near the threshold energy or is simply an artifact of the potential remains to be explored further. At this stage, it is difficult to compare our calculated reaction probabilities with those obtained by the RBU model of Yu and Nyman.[28] Since the RBU model is based on the collinear collision approach, its calculated reaction probabilities are much larger than the present result as given in ref 28. We believe that the current SVRT reaction probabilities are more realistic because the overall spatial rotation of the collision system is treated more accurately.

For calculation with total angular momentum $J > 0$, the CS (centrifugal sudden) approximation is employed and the dynamics calculation is carried out for J up to 124. These calculations yield total integral cross sections from the initial ground-state according to the standard formula

$$\sigma_{00}(E) = \frac{\pi}{k^2}\sum_J (2J+1)P_{00}^J(E) \qquad (14)$$

Figure 6 shows the integral cross section as a function of translational energy. The calculated cross section on the C-T PES (dotted line) is much smaller than that on the JG PES (solid line), as shown in the figure. For comparison, we also plotted the cross section calculated by Clary using a 3D RBA approximation[26] in Figure 6. The RBA cross section (dot−dashed line) is calculated on the C-T PES and is much larger than the present SVRT result on the same PES, as shown in Figure 6. It is interesting to note that both calculations are carried out on the same C-T surface but using two difference dynamical methods. Thus, the difference in two results is entirely due to the difference in dynamical models employed. One possible reason for this divergence is perhaps that the RBA method

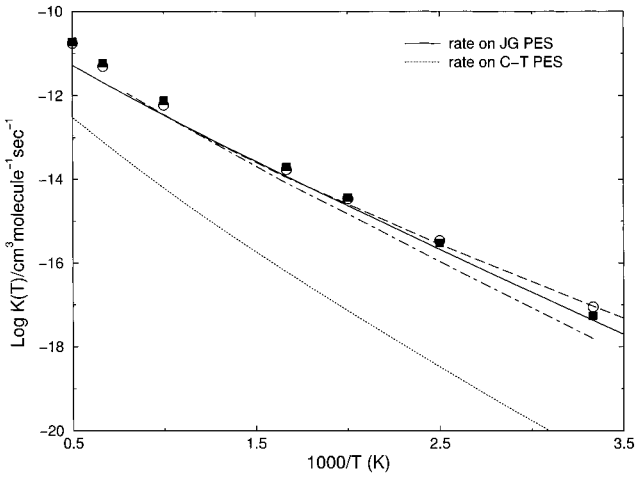

Figure 7. Comparison of calculated rate constants with the experimental results for the reaction $O(^3P)+CH_4 \rightarrow OH + CH_3$. The solid line is our calculated result on JG PES and the dotted line is that on C-T PES. The RBU result of Yu and Nyman[28] is given as long-dashed line and the RBA result of Clary[26] is shown as dot−dashed line. The circles and squares denote, respectively, the experimental results of refs 17, 20 and 18, 19.

mainly samples the most favorable configuration for reaction, i.e., collinear approach; it therefore may overestimate the cross section. Investigation of the C-T surface shows that the reaction barrier of the C-T surface rises quickly as the system moves away from collinear configuration. In the SVRT model, the spatial orientation of the collision system is treated correctly; it is therefore expected to give a more accurate description of the stereodynamics as is demonstrated in a previous study of the $H + H_2O$ reaction.[15]

We also calculate the reaction rate constant from the initial ground state of the reagent using the formula

$$r_{00}(T) = \left(\frac{8kT}{\pi\mu}\right)^{1/2}(kT)^{-2}\int_0^\infty dE_t\, E_t \exp(-E_t/kT)\sigma_{00}(E_t) \qquad (15)$$

For the $O(^3P) + CH_4$ reaction there is a Jahn−Teller conical intersection along the collinear O−H−CH_3 geometry, which causes the splitting of the electronic state. As a result, the electronic state is split into two electronic states of symmetries $^3A'$ and $^3A''$.[21,22] It is assumed that $^3A'$ and $^3A''$ states contribute almost equally to the reaction $O(^3P) + CH_4$.[21] Following the practice of refs 26, and 28, our calculated rate constant is multiplied by an extra factor of 2 in order to compare with experiment. Figure 7 shows that the rate constant calculated on the C-T surface is orders of magnitude smaller than that calculated on the JG surface. The latter rate constant is in good agreement with experimental measurements especially at low temperatures. The theoretical results using RBA and RBU methods on the C-T surface are also plotted in Figure 7 for comparison. These rate constants seem to be in close agreement with the current SVRT result on the JG surface. Because different dynamical approximations are employed in different methods, more extensive studies need to be carried out to examine the validity and accuracy of these results.

The results of current dynamics calculation show that the C-T surface gives too little reaction. The main reason for insufficient reactivity of the C-T surface is not because its barrier is too high, but rather the incorrect topology of the potential surface in and near the interaction region. The C-T surface was constructed on the basis of dual level quantum chemistry calculations and was calibrated using variational transition state calculations of rate constant.[21] However, there are problems with

this approach. First, the TST theory does not depend on the global feature of the potential, it only explores the saddle point and/or reaction path. Second, various transition state methods do not give results that agree with each other.[21] This approach is especially problematic when the accuracy of ab initio calculation is not very high as in the case of C-T surface.[21] Since the transition state calculation does not include global properties of the surface, it is not surprising to see that the global contour lines of the C-T PES look awkward and "bend" away instead of toward the transition state, as shown in Figure 3.

The C-T PES is constructed from the same functional forms as the GJ surface but its parameters are chosen on the basis of TST calculations without extensive dynamics calculations. Since the current study uses the same SVRT model to perform dynamics calculations on both surfaces, the drastic difference in dynamics result must be due to the topological difference of the two surfaces. Contour plots of the two surfaces show that the main difference between the two surfaces is not in the transition state but near the entrance toward the transition state. This difference in surface results in different dynamical behavior, which can only be detected from dynamics calculations but not from transition state calculations. Although the current SVRT model does not include all dynamical degrees of freedom and the full effect of these neglected degrees of freedom on dynamical result is unknown, the fact that the same model yields quite different results on two seemingly similar surfaces gives strong support for the above analysis. Of course, the reader should keep in mind that the SVRT model is approximate and our result needs to be verified by future more exact theoretical studies.

IV. Conclusion

The 4D SVRT model has been applied to study the reaction $O(^3P)+CH_4 \rightarrow CH_3 + OH$. Time-dependent quantum wave packet calculations have been carried out for the title reaction on the C-T PES and on the JG PES, which is originally constructed for the $H + CH_4$ reaction. In the SVRT model, the C−H bonds and the bond angle α of group $H-CH_3$ are fixed at its transition state and the dynamics calculation involves only four mathematical dimensions. Reaction probabilities, cross sections and rate constants from the initial ground state are calculated. The energy dependence of reaction probability shows a tunneling effect. In particular, the rate constants calculated on the JG PES are in quite good agreement with experimental measurements. However in comparison, the C-T surface gives too little reactivity. In addition to having a slightly higher reaction barrier, the shape of contour lines of the C-T surface "bends" toward the "wrong" direction and is responsible for reflecting the wave packet back to the entrance channel.

Our dynamics calculation clearly shows that the C-T PES is inadequate and needs to be improved globally. This investigation demonstrates the importance of the global effect of a potential surface on reaction dynamics. It emphasizes the importance and need of using the dynamics method to check and calibrate a global potential surface, especially if the accuracy of ab initio calculation is not sufficiently high. Rate constant calculations using transition state theory alone are often insufficient to determine a global potential surface.

Acknowledgment. J.Z.H.Z. is supported by the National Science Foundation and the Petroleum Research Fund. We thank Prof. Gunnar Nyman and Dr. J. C. Corchado for sending us copies of JG and C-T PES, respectively.

References and Notes

(1) Zhang, J. Z. H.; Dai, J.; Zhu, W. *J. Phys. Chem. A* **1997**, *101*, 2746 and references therein.
(2) Manthe, U.; Seideman, T.; Miller, W. H. *J. Chem. Phys.* **1993**, *99*, 10078.
(3) Neuhauser, D. *J. Phys. Chem.* **1994**, *100*, 9272.
(4) Zhang, D. H.; Zhang, J. Z. H. *J. Chem. Phys.* **1994**, *101*, 1146.
(5) Zhang, D. H.; Light, J. C. *J. Chem. Phys.* **1996**, *104*, 4544.
(6) Zhu, W.; Dai, J. Q.; Zhang, J. Z. H.; Zhang, D. H. *J. Chem. Phys.* **1996**, *105*, 4881.
(7) Pogrebnya, S. K.; Echave, J.; Clary, D. C. *J. Chem. Phys.* **1997**, *107*, 8975.
(8) Sun, Q.; Bowman, J. M. *J. Chem. Phys.* **1990**, *92*, 5201.
(9) Brook, A. N.; Clary, D. C. *J. Chem. Phys.* **1990**, *92*, 4178.
(10) (a) Bowman, J. M.; Wang, D. *J. Chem. Phys.* **1992**, *96*, 7852. (b) Wang, D.; Bowman, J. M. *J. Chem. Phys.* **1992**, *96*, 8906.
(11) (a) Clary, D. C. *J. Chem. Phys.* **1991**, *95*, 7298; (b) **1992**, *96*, 3656.
(12) Szichman, H.; Last, I.; Baram, A.; Baer, M. *J. Phys. Chem.* **1993**, *97*, 6436.
(13) Balakrishnan, N.; Billing, G. D. *J. Chem. Phys.* **1994**, *101*, 2785.
(14) Zhang, J. Z. H. *J. Chem. Phys.* **1999**, *111*, 3929.
(15) Zhang, D. H.; Zhang, J. Z. H. *J. Chem. Phys.* **2000**, *112*, 585.
(16) Wang, M. L.; Li, Y. M.; Zhang, J. Z. H.; Zhang, D. H. *J. Chem. Phys.* **2000**, *113*, 1802.
(17) Baulch, D. L.; Cobos, C. J.; Cox, R. A.; Esser, P.; Frank, P.; Just, Th.; Kerr, J. A.; Pilling, M. J.; Troe, J.; Walker, R. W.; Warnatz, J. *J. Phys. Chem. Ref. Data* **1992**, *21*, 445.
(18) Cohen, N. *Int. J. Chem. Kinet.* **1986**, *18*, 59.
(19) Cohen, N.; Westberg, K. R. *Int. J. Chem. Kinet.* **1986**, *18*, 99.
(20) Sutherland, J. W.; Michael, J. V.; Klemm, R. B. *J. Phys. Chem.* **1986**, *90*, 5941.
(21) Corchado, J. C.; Espinosa-Garcia, J.; Roberto-Neto, O.; Chuang, Y. Y.; Truhlar, D. G. *J. Phys. Chem. A* **1998**, *102*, 4899.
(22) Espinosa-Garcia, J.; Garcia-Bernaldez, J. C. *Phys. Chem. Chem. Phys.* **2000**, *10*, 2345.
(23) Gonzalez, M.; Hernando, J.; Millan, J.; Sayos. *J. Chem. Phys.* **1999**, *110*, 7316.
(24) Neto, O. R.; Machado, F. B. C.; Truhlar, D. G. *J. Chem. Phys.* **1999**, *111*, 7326.
(25) Yu, H. G.; Nyman, G. *J. Chem. Phys.* **1999**, *111*, 3508.
(26) Clary, D. C. *Phys. Chem. Chem. Phys.* **1999**, *1*, 1173.
(27) Palma, J.; Clary, D. C. *J. Chem. Phys.* **2000**, *112*, 1859.
(28) Yu. H. G.; Nyman, G. *J. Chem. Phys.* **2000**, *112*, 238.
(29) Jordan, M. J. T.; Gilbert, R. G. *J. Chem. Phys.* **1995**, *102*, 5669.
(30) Zhang, J. Z. H. *Theory and Application of Quantum Molecular Dynamics*; World Scientific: Singapore, 1998.
(31) Fleck, J. A.; Morris, J. R., Jr.; Feit, M. D. *Appl. Phys.* **1976**, *10*, 129.
(32) Warnatz, J. In *Combustion Chemistry*; Gardiner, W. C., Ed.; Spriger-Verlag: New York, 1984; p 233.